

# Optimising simulated commercial paper for pulp quality analysis.

R. J. N. HELMER<sup>\*</sup>, G. H. COVEY<sup>~</sup>, W. D. RAVERTY<sup>□</sup>, AND N. VANDERHOEK<sup>‡</sup>.

<sup>\*</sup>Postgraduate student, The University of Melbourne, Parkville, Vic. 3052 Australia.

<sup>~</sup> General Manager Covey Consulting

<sup>□</sup> Director, Paper Science,

PO Box 424, Rosanna, Vic. 3084 Australia.

<sup>‡</sup>Technology Manager: Fine Papers, Amcor R&T, Private Bag 1, Fairfield, Vic. 3078 Australia.

## SUMMARY

The formation potential of two short fibre pulps, a bleached Tropical Hardwood Kraft (THK), and a bleached Eucalypt Kraft, (BEK), were investigated. Sheets were formed at various consistencies and velocities consistent with commercial operation on the UoM former. The sheets formed during the study were assessed by standard commercial tests which included an ultrasonic test for anisotropy and a beta-ray formation test. The flow conditions were found to be very important for optimising the forming potential of a given pulp. Both of the pulps investigated exhibited an optimum formation, but at different process conditions. The results suggested that an optimum flow condition exists for obtaining the best formation from a given pulp. The BEK pulp was found to have a superior forming potential. These results may be extrapolated to suggest target, idealised flow conditions for forming paper on commercial papermachines. Furthermore, a tool has been developed by which the performance of pulps under machine conditions may be predicted with more confidence in the laboratory.

## INTRODUCTION

Analysis of the forming potential of many pulp stocks has largely been restricted to sheets formed using a standard handsheet former, one of a number of assorted laboratory formers, or through expensive pilot scale trials. Standard handsheet and conventional laboratory forming devices generally have forming conditions which are far removed from the commercial process (1-16). None of these devices has been deemed to be a truly satisfactory predictor of what may be expected on a commercial machine from a given fibre stock. Hence, predicting the performance of new furnishes at commercial process conditions has been difficult. The production of paper in the laboratory where controlled forming conditions result in an anisotropic sheet of predictable properties, which match those of papers made on a commercial paper machines, has been a long desired instrument for many researchers.

The University of Melbourne laboratory former (UoM) produces an anisotropic sheet of paper with repeatable properties (17). Controlled forming conditions result in laboratory sheets with properties which match those

properties of papers made on commercial paper machines at similar operating conditions (*same* consistency with an equivalent jet to wire velocity, depth and vacuum profile). The laboratory sheet former simulates commercial processes by employing a novel interpretation of the flow in the forming region resulting in a system where stock flows over a stationary wire, (with a free upper surface).

## THEORY

The fibre orienting effect of the rush/drag ratio is well documented (18, 19). Reports of investigations into sheet anisotropy, and specifically MD/CD fibre orientation have repeatedly stressed that the rush/drag ratio is a key determinant of the degree of fibre orientation. The effect of jet to wire ratio on fibre orientation has been re-interpreted to be more accurately expressed as arising from the velocity difference between the jet emerging from the headbox and the velocity of the wire (19, 20). This observation formed the basis for the conceptual design of the current apparatus.

The conceptual analogy used for the design of the UoM stationary wire was similar to the “moving with the flow” type analogy often used in fluid dynamics where a frame of reference with a mean velocity is used to convert a spatial domain into a temporal one. The mean reference velocity applied in this case is the speed of the wire,  $V_w$  (m/s). The analogy used for the design of the UoM laboratory model is depicted below in figure 1.

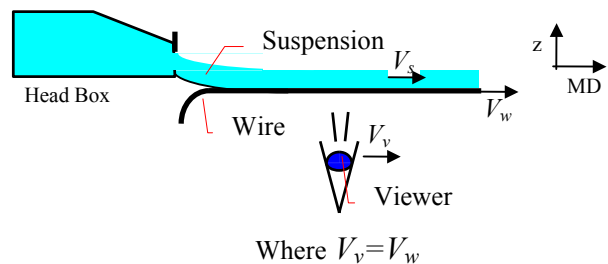


**Figure 1. The model's analogy, (where  $V$  = velocity (m/s) and subscripts,  $s$  = suspension,  $w$  = wire, and  $v$  = viewer).**

The key wet-end features of the UoM include: a velocity profile above the wire, similar suspension characteristics, (similar consistency range and depth), and a similar pressure profile. The stationary wire concept has a simple relation between the commercial process operating parameters and the laboratory operating parameters. The known machine parameters were related to the laboratory parameters of the conceptual stationary wire former to achieve a 1:1 scale by equations 1.1 to 1.5.

$$c_{LF} = c_{CM} \quad \text{Eq. 1.1}$$

$$h_{LF} = h_{CM} \quad \text{Eq. 1.2}$$

$$\bar{v}_{LF} = V_{CM} \times |R_{CM} - 1| \quad \text{Eq. 1.3}$$

$$P_{LF}(t) = P_{CM}(x) \times V_{CM} \quad \text{Eq. 1.4}$$

$$t_{LF} = \frac{L_{CM}}{V_{CM}} \quad \text{Eq. 1.5}$$

where,

- $c$ , consistency, ( $w/w$  %),
- $h$ , height over wire, (m),
- $\bar{v}$ , suspension velocity, (m/s),
- $V$ , machine speed (wire), (m/s)
- $R$ , jet to wire ratio,
- $P$ , vacuum pressure, (kPa),
- $t$ , forming time, (s), and,
- $L$ , dry line position, (m).

The subscripts  $LF$  and  $CM$  refer to the laboratory former and commercial machine respectively. The model similitude is discussed further elsewhere (21).

### APPARATUS

The principle components of the UoM sheet former include:

1. a novel multi-slice headbox ( $CD_y$  width 400mm),
2. a large single pulse vacuum box ( $MD_x$  forming length 500mm,  $CD_y$  width 400mm),
3. a 110L head tank,
4. a 110L receiver tank
5. a customised, reducing diameter, bifurcated distributor,
6. a large vacuum reservoir,
7. a centripetal pump.
8. a plate to support the flow prior to forming arranged in a manner so that the support is withdrawn rapidly,
9. a self supporting flow receiver with fixed transparent walls which extend right up to the headbox,
10. a fast closing gate valve to halt the flow, and,
11. an automated integrated control system.

The components were assembled as shown in Figure 2 below, to establish a re-circulating flow loop.

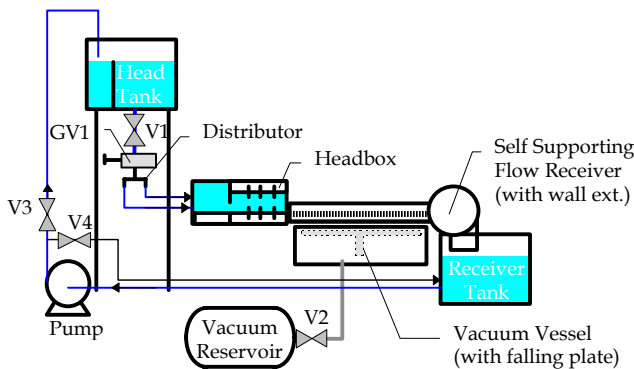


**Figure 2: Schematic diagram of the basic components and the configuration of the laboratory former.**

The de-watering was controlled by an automated integrated control system employing an electronically timed, pneumatically actuated, mechanical control system as shown in figure 3. The control system was discussed in an

earlier paper (17). Forming was initiated by the electronically controller.

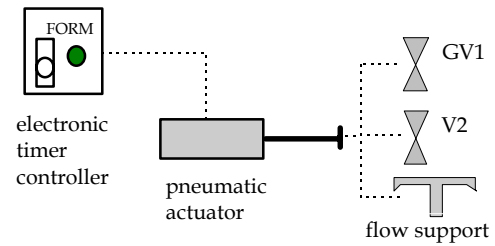


**Figure 3: UoM Integrated Control Scheme**

### PROCEDURE

#### Experimental Strategy.

The commercial process conditions for optimum paper properties vary from machine to machine due to inherent differences. The operating conditions used commercially for fine paper production with Fourdrinier (and hybrid) machines typically lie within the range shown in Table 1.

**Table 1  
Typical Commercial Operating Conditions for Fourdrinier (and hybrid) papermachines.**

Process Variable	Units	Range
Consistency, $c$	$w/w$ %	0.3 to 0.8
Velocity <sup>1</sup> , $\Delta V_{JW}$	m/s	-0.6 to +0.6

The strategy employed in this process investigation of the effect of velocity and consistency on paper properties was to form sheets on the UoM former at conditions consistent with the range shown in table 1 for two nominally similar short fibre pulps. A comparison of the relative quality potential of the pulps at similar process conditions could then be effected. Sheets were formed using the UoM laboratory former from BEK and THK pulps at various operating conditions within the range shown in Table 2.

**Table 2  
UoM Operating Conditions.**

Pulp	Operating Range	
	$c$ ( $w/w$ %)	$\bar{v}$ (m/s)
THK	0.3 to 0.83	0.3 to 0.7
BEK <sup>2</sup>	0.5	0.22 to 0.63

This investigation was a part of a wider process variable study and it was only possible to form sheets with the BEK at one consistency as only very small amounts of pulp were available (~1.2 kg).

#### UoM Sheet Forming.

<sup>1</sup> “+ = rush”, a higher jet speed relative to the wire.

<sup>2</sup> It was not possible to study this pulp over a wider consistency range as earlier studies had used large amounts of this pulp and it was no longer available as dry lap.

The initial UoM settings for THK were as shown in Table 3. A similar system was established for the BEK but with less pulp.

**Table 3**  
**Initial UoM Machine Parameters, THK.**

Parameter	Value	Precision
Slice Height	10 mm	± 0.25 mm
System Head	1 m-stock	± 0.01 m
Vacuum Time	0.6 s	± 0.02 s
Reservoir Vacuum	50 kPa (gauge)	± 0.5 kPa
Mass of Pulp	1.7 kg	± 0.01 kg
System Volume	210 L	± 5 L

The settings in table 3 resulted in a peak vacuum in the process vacuum vessel  $\Delta P_{max} = -8$  kPa, and a flow depth above the wire,  $h = 10$  mm. UoM sheet forming required the establishment of a stable flow loop, subsequent sampling and recording of the process variables, followed by the operator activating the electronic control system. Process changes to the consistency and velocity were effected by diluting the system and adjusting valve V1, (see figure 2) respectively.

The wet sheets were couched on to sheets of blotting paper (~200 gsm, 42 x 57 cm<sup>2</sup>) with a layer of thin woven nylon mesh interposed between the wet sheet and the blotting paper to facilitate separation of the sample and the blotting paper after drying. Further de-watering was achieved by pressing manually against additional dry blotting paper with a hand roller. No other pressing was used. The sheets were allowed to dry freely in open conditions. A number of sheets were formed at each operating condition. Further UoM operational details are discussed elsewhere (17, 21).

**Pulp Stocks.**

Two air dried, un-refined, dry lapped short fibre pulps were used in this investigation, a bleached Tropical Hardwood Kraft (THK), and a bleached Eucalypt Kraft (BEK) pulp. The fibre characteristics of these pulps shown in Table 4 were measured using a Kajaani FS-200.

**Table 4**  
**Fibre Characteristics of THK and BEK Pulp.**

Pulp		THK	BEK
Fibre Length	(mm)	0.82	0.81
Fibre Coarseness	(mg/m)	0.099	0.115

The stocks were prepared by suspending measured quantities of pulp in measured volumes of town water. A small amount of commercial sodium hypochlorite was added to prevent bacterial growth, (10 ml into the 200L system).

**Process Variable Measurement.**

Stock consistencies were measured gravimetrically by sampling directly from the flow receiver and filtering through pre-weighed, oven dry, analytical filter paper, (Whatman No. 541). The filter cake was then oven dried (110°C) for 12 hrs before subsequent weighing.

A mean stock velocity over the wire was determined by measuring the time taken for a neutrally buoyant particle to traverse the forming region (0.5m).<sup>3</sup>

The pressure differential profile within the suction box was recorded by a pressure transducer located within a side port and logged to a computer. The software was set to log the pressure data every 10ms over a 3s interval from the point of initiation<sup>3</sup>.

**Sheet Analysis.**

A4 samples were cut from the central region of highest uniformity. The dimensions of this region are provided below in figure 4.

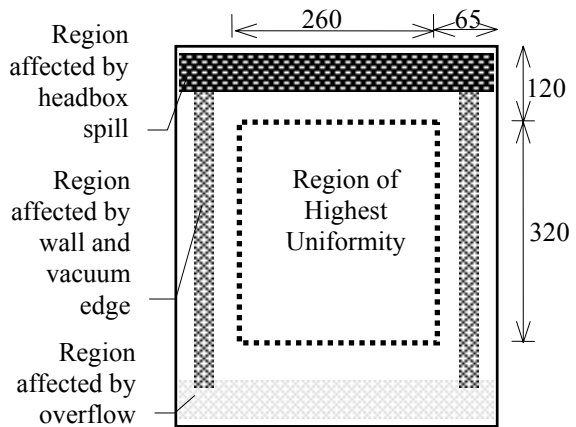


**Figure 4: Crude sheet produced on the Mk II former with the region of uniformity identified.**

The planar nature of paper means that a sheet may be reasonably characterised by its formation and MD-CD fibre orientation distribution. It is likely that these sheet characteristics are interrelated (22).

Formation was measured using beta-radiography (Ambertec Model No. BFT-1) and the common formation indices were employed to characterise formation.

Coefficient Of Variation, COV:

$$COV = \frac{\sigma}{B_{Wt}} \tag{Eq 2.1}$$

and,

Normalised Formation Index, NFI:

$$NFI = \frac{\sigma}{\sqrt{B_{Wt}}} \tag{Eq 2.2}$$

where,

<sup>3</sup> This measurement method is representative of the mean velocity for a plug flow, see (21).

<sup>3</sup> the typical forming time was of the order of 0.2s as determined by image analysis.

$B_{wt}$ , Basis weight/grammage, (gsm), and,  
 $\sigma$ , standard deviation of basis weight (gsm).

An aperture size of 1mm with a scanning region of 69 x 69 mm<sup>2</sup> was employed. This device is reported to be the most accurate (23) with an error of 0.25 gsm (24).

Sonic velocity measurements were performed using a Nomura Shoji (Model No. FST 3000). The resulting fibre orientation index, FOI is the ratio of the maximum ( $u_{max}$ ) and minimum ( $u_{min}$ ) sonic velocities<sup>4</sup>:

$$FOI = \frac{u_{max}}{u_{min}} \quad \text{Eq 2.3}$$

where,

$u$ , sonic velocity, (km/s).

## RESULTS

### Bleached Eucalypt Kraft, BEK.

All of the BEK sheets were formed at  $c = 0.5$  w/w % and the sheets' characteristic indices are shown in figures 5 to 7 with respect to *velocity*. Note the instability at  $\bar{v} = 0.32$  m/s was due to a change in the channel flow regime, ( $Fr \sim 1$ , see (21)).

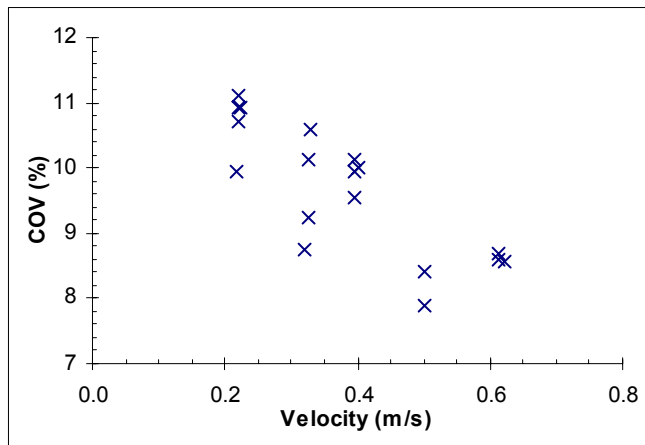


Figure 5: COV of BEK sheets at  $c = 0.5$  w/w % and various velocities, ( $h = 10$ mm,  $\Delta P_{vac} = -8$ kPa).

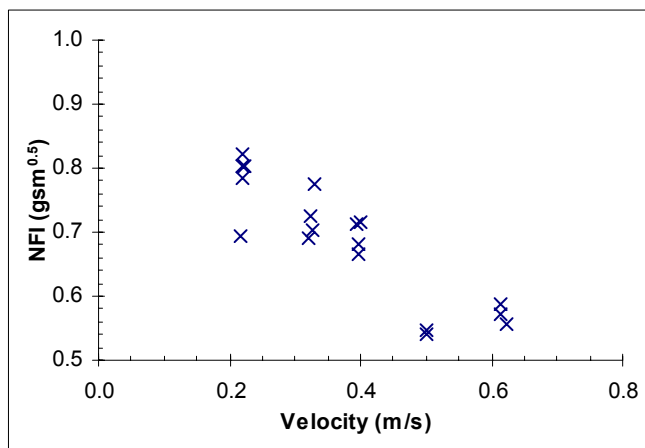


Figure 6: NFI of BEK sheets at  $c = 0.5$  w/w % and various velocities, ( $h = 10$ mm,  $\Delta P_{vac} = -8$ kPa).

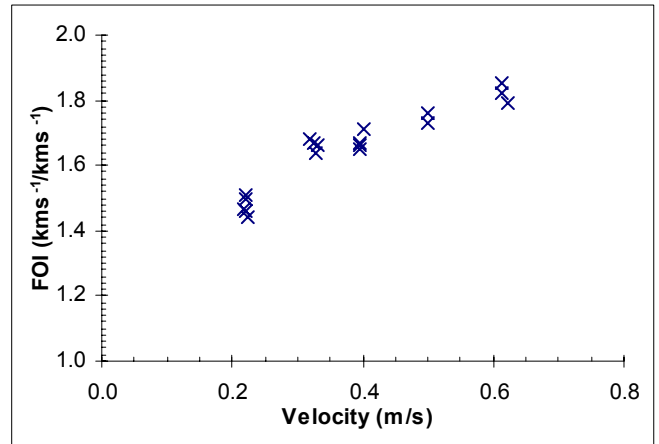


Figure 7: FOI of BEK sheets at  $c = 0.5$  w/w % and various velocities, ( $h = 10$ mm,  $\Delta P_{vac} = -8$ kPa).

### Bleached Tropical Hardwood Kraft, THK.

The THK results are shown in figures 8 to 10 and appendix A, figures A1 to A6 and Table A1 with respect to *consistency*.

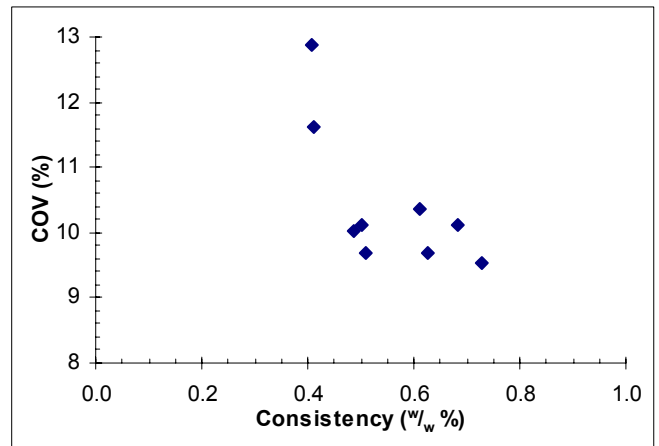


Figure 8: COV of THK sheets at  $\bar{v} = 0.4$  m/s and various consistencies, ( $h = 10$ mm,  $\Delta P_{vac} = -8$ kPa).

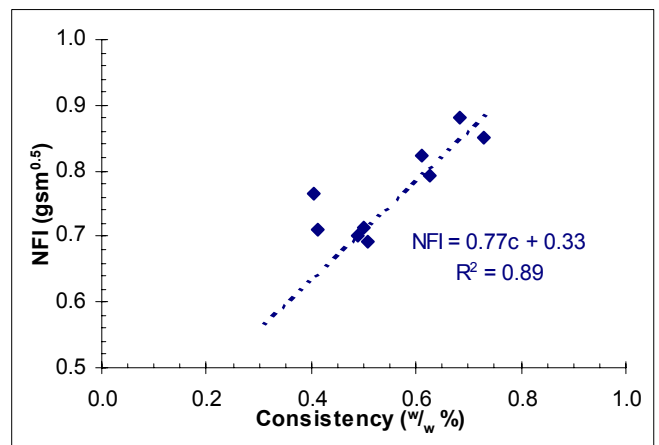


Figure 9: NFI of THK sheets at  $\bar{v} = 0.4$  m/s and various consistencies, ( $h = 10$ mm,  $\Delta P_{vac} = -8$ kPa).

<sup>4</sup> The MD/CD and Max/Min ratios were very similar.

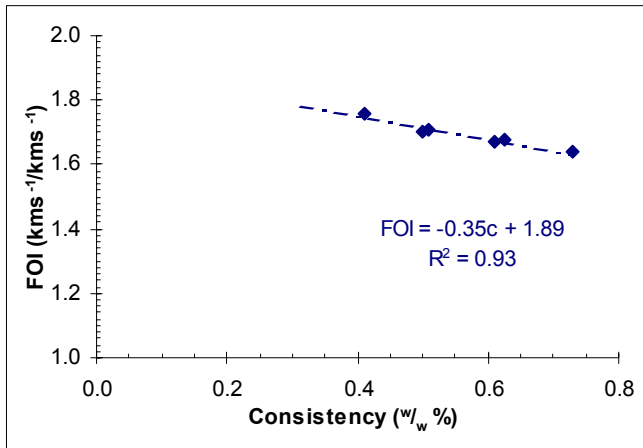


Figure 10: FOI of THK sheets at  $\bar{v} = 0.4$  m/s and various consistencies, ( $h = 10$ mm,  $\Delta P_{vac} = -8$ kPa).

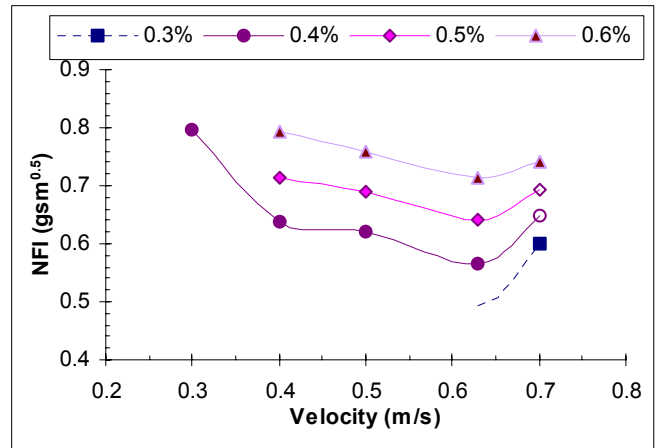


Figure 11: NFI of THK at four consistencies and various velocities, ( $h = 10$ mm,  $\Delta P_{vac} = -8$ kPa).<sup>7</sup>

## DISCUSSION

### Operating Conditions.

The flow conditions were found to be very important for optimising the forming potential of a given pulp. A summary of the limits imposed on the operating conditions derived from the THK investigation is shown in figure 10, the limits are discussed elsewhere (21).

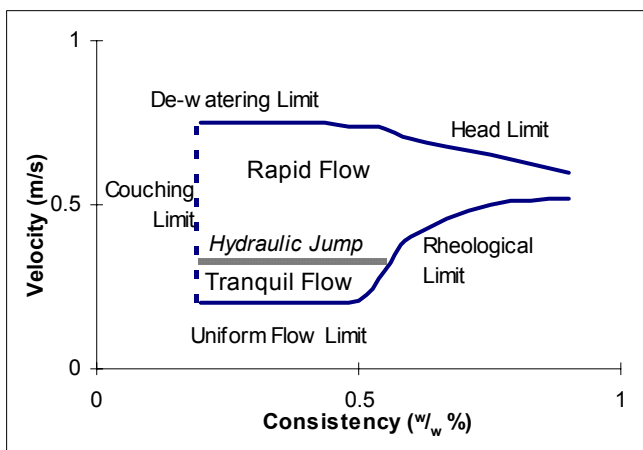


Figure 10: UoM Laboratory Former Operational Limits, (THK).

### The Effect of Velocity.

The effect of velocity<sup>5</sup> on formation was complex and an optimum formation was observed at an intermediate velocity, see figures 5 and 6 for BEK, and is summarised in figure 11 for THK<sup>6</sup>. The behaviour was consistent with commercial Fourdrinier machines where an optimum formation is observed at jet to wire differences of ca 15 -25 m/min (0.25 - 0.42 m/s), (higher jet to wire velocity differences lead to poorer formation).

The effect of velocity increases on the MD fibre alignment was also consistent with that observed on commercial Fourdrinier machines, see figure 7 for BEK and figure 12 for THK. The fibre orientation was significantly affected by the velocity at low velocities. However, a plateau was reached at higher velocities and only small increases were then observed. This behaviour is consistent with both pilot machine studies (19) and commercial data (20). The plateau occurred after the flow changed from a tranquil flow to a rapid flow, (at  $\bar{v} \geq 0.32$  m/s, see (21)).

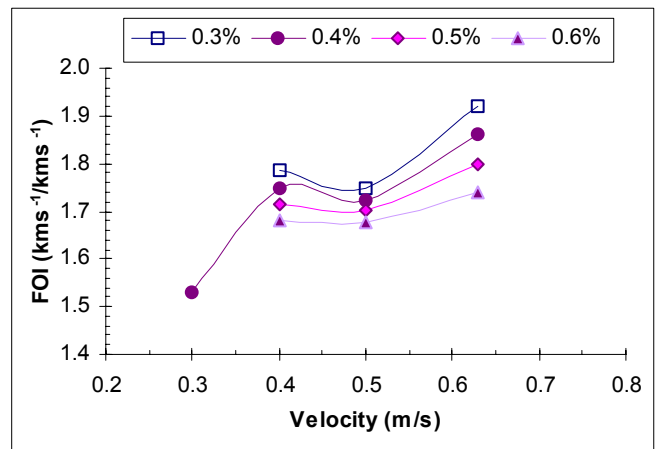


Figure 12: FOI of THK at four consistencies and various velocities, ( $h = 10$ mm,  $\Delta P_{vac} = -8$ kPa).

### The Effect of Consistency.

The analysis of the effect of consistency was complicated by the need to compare sheets with different basis weights. The COV data suggested that the formation was largely independent of stock consistency above 0.4 w/w %, (within the  $c$  range investigated, see figures A1, A4, and Table A1.1), except at very high velocity, (see figure 8). Below 0.4 w/w % the COV was markedly higher indicating significantly poorer formation. However, the NFI exhibited a near linear improvement with decreasing consistency until ca 0.4 w/w % where it began to increase, again indicating poorer formation at low consistency, (see figures

<sup>5</sup> Even though the sheets had similar basis weights.

<sup>6</sup> COV trend is similar.

<sup>7</sup> The hollow points were obtained from interpolation.

9, A2, A5, 12 and Table A1.1). The COV behaviour was in stark contradiction to the generally accepted notion that lower consistencies lead to improved formation. It was observed that there was a change in the flow behaviour of the THK suspension at ca 0.4 % with considerably more individual fibre motion indicating greater turbulence. The scale of this turbulence was observed to be of the order of a few fibre lengths.

The FOI exhibited a linear decrease with increasing consistency but the interpretation of the effect was complicated by the simultaneous basis weight increases, (see figures 10, A3, A6, 12 and Table A1.1) . The top side and wire side fibre alignment of Fourdrinier machines is quite different (25). The UoM exhibited a similar two sidedness (17). The two sidedness of the sheets complicates the interpretation of the FOI's which represent a mean fibre alignment for the sheet. The effect of the consistency was thus somewhat masked by the differences in basis weight (i.e. a reduced wire side contribution in a thicker sheet might have led to lower FOI's for sheets formed at higher consistency)<sup>8</sup>. The fibre alignment in individual layers of sheets formed at different consistencies might be somewhat similar and thus independent of consistency within the range investigated here. However, it may also be consistent with the notion that higher consistencies lead to more "felted" sheets (25). Further analysis is required.

#### Comparison of BEK and THK.

A comparison of the formation of sheets formed over a range of velocities at the same consistency, flow depth and vacuum application for the two pulps investigated is shown in figure 13. Both of the pulps investigated exhibited an optimum formation, but at different process velocities. At low velocities the THK and BEK exhibited very similar formation. However, the pulps behaved quite differently at higher velocities.

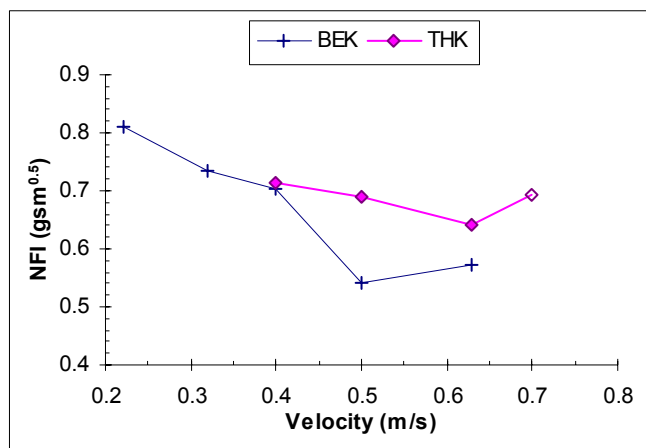


Figure 13: Comparison of the forming potential of THK and BEK over a range of velocities at  $c = 0.5$  % w/w.

<sup>8</sup> Note that the sheets formed at different velocities and constant consistency had similar basis weights and so the two sidedness of the sheets was not a concern for those results.

The optimum formation of BEK sheets was better than the THK and achieved at a lower velocity. Hence, the BEK appeared to have a superior formation potential and thus be a superior quality pulp. The effect of the velocity suggested that a pulp's response to flow conditions was an important factor which determined the potential formation<sup>9</sup>.

The extent of MD fibre alignment of BEK and THK was similar although the BEK FOI was generally slightly higher, see figure 14.

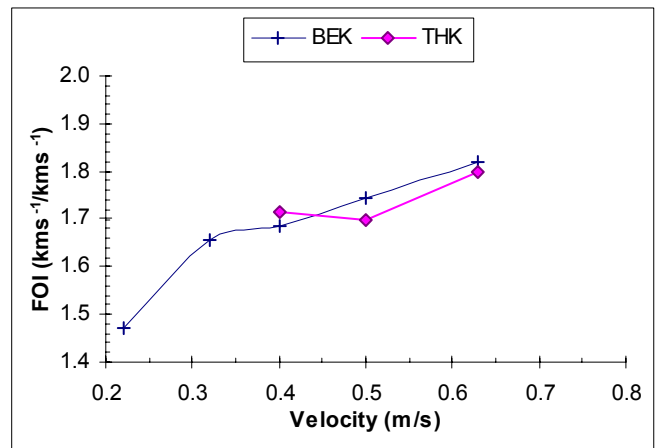


Figure 14: Comparison of the forming potential of THK and BEK over a range of velocities at  $c = 0.5$  % w/w.

The fibre orientation angles were in the range (0±3°) indicating a low level of cross flow on the wire of the UoM former. The formation and fibre orientation indices are consistent with those observed for similar papers made on commercial paper machines (22, 26). The NFI formation index (26) has been correlated with a fibre crowding number for a number of stocks produced on a Fourdrinier paper machine (fine paper  $R^2=0.64$ ). The distinct trends exhibited by the NFI for the various forming conditions has led to an empirical model which predicts the formation of sheets formed on the UoM laboratory former with various pulp stocks at various operating conditions, ( $R^2=0.8$ ). The correlation will be presented in a later paper.

The UoM laboratory former has been used to form sheets with formation and fibre orientation indices which are very similar to those of papers made on full scale paper machines at similar operating conditions. Further work to explore the effect of pulp characteristics on sheet characteristics and gain further insights is in progress.

#### CONCLUSION

The UoM laboratory former has differentiated between two nominally similar pulps and has explored the forming potential of each pulp. The measured effect of changes in consistency and forming velocity were consistent with those found on commercial Fourdrinier formers. The BEK was found to have a superior forming potential to the THK.

<sup>9</sup> Unfortunately, due to exhausted supplies, it was not possible to form sheets with BEK over a wide consistency range and the comparison has been limited to velocity.

## ACKNOWLEDGMENTS

The authors wish to thank:

- Amcor Limited for use of testing equipment, library resources, provision of pulp samples, loan of experimental equipment from its Research and Technology (R&T) Centre, and technical advice.
- staff of Amcor R&T for helpful advice.
- Albany for the forming wire material.
- The University of Melbourne Department of Chemical Engineering Workshop.
- DEET for APAi funding.
- CSIRO for sustenance.

✉

## REFERENCES

1. Lindberg, N. J.; "The sheet formation and new Investigation Possibilities I", *Paperi ja puu*, **34** (6): 275 (1952).
2. Lindberg, N. J.; "The sheet formation and new Investigation Possibilities II", *Paperi ja puu* **34** (7): 227 (1952).
3. Lindberg, N. J.; "The sheet formation and new Investigation Possibilities III", *Paperi ja puu*, **34** (8): 287 (1952).
4. Nordman, L.; "Laboratory investigation of water removal by a dynamic Suction box", *Tappi J.*, **37** (11): 553 (1954)
5. Steenberg, B., Bergström, J., and Kjensjord, R. I.; "Model experiments of sheet formation on the cylinder wire", *Sv. Pappstidn*, **58** (2) : 40 (1955).
6. Toroi, M.; "The preparation of fibre oriented sheets on a laboratory scale", *Paperi ja puu*, **41** (5): 271 (1959).
7. Prusas, Z. C.: "Laboratory study of the effects of fibre orientation on sheet anisotropy", *Tappi J.*, **46** (5): 325 (1963).
8. Rytö, N., Aaltonen, P., Perttilä, T, and Talja, M.; "Device for the production of fibre-oriented laboratory handsheets", *Paperi ja puu*, **51** (3): 207 (1969).
9. Moller, K., Jönsson, L., and Ek, R., "A new handsheet former simulating Fourdrinier Forming", *Sv. Pappstidn* **82** (9) : 267 (1979).
10. Trepanier, R. J., "Dynamic Forming: Parameters for making oriented sheets in the laboratory", *Pulp and Paper Canada*, **90** (4) : 45 (1989).
11. Ting, T., "The Dynamic Former: Principles of Paper Making", *APPI Handout*, (1996).
12. Koran, Z., and Kabamba, M., "Fibre orientation indices from standard tests", *Proc. Tappi 1987 Paper Physics Conf.*, 193 (1987).
13. Kärtilä, S., Räisänen, K., and Paulapuro, H.; "The moving Belt Drainage Tester (MBDT)", *Proc. Tappi 1992 Papermakers Conf*, 275 (1992).
14. Räisänen, K., Paulapuro, H., and Maijala, A.; "Effect of vacuum level and suction time on vacuum assisted drainage of a papermachine wire section", *Appita J.* **48** : (4), 269, (1995).
15. M/K Systems Inc., "Accessories for the M/K sheet former, as well as other handsheet machines", product information, (care of Hans Nilsson), (1997).
16. Xu, L., and Parker, I., "Simulating the forming process with the Moving Belt Drainage Former", *Proc. 53rd Appita Annual Conf.*, Vol. I., 169 (1999).
17. Helmer, R. J. N., Covey, G. H., Raverty, W. D., and Vanderhoek, N., "Preliminary development of a laboratory former for oriented sheets", *Proc. 53rd Appita Annual Conf.*, Vol. I., 79 (1999).
18. Wiklund, L. G.: "Pappersmaskinens inflytande på papperets egenskaper." *Norsk Skogindustri.*, **2** : (3) 69 (1948).
19. Niskanen, K. J.; "Distribution of fibre orientations in paper", *The Pulp and Paper Fundamental Research Society*, 275 (1989).
20. Condon, M.; "Mechanical aspects of forming and formation, a current review", *Proc. 1996 Tappi Papermaker's Conf.*, 253 (1996).
21. Helmer, R. J. N., Covey, G. H., Raverty, W. D., and Vanderhoek, N., "Flow phenomena and paper forming" *Proc. 54th Appita Annual Conf.*, (1999).
22. Hasuike, M., Johansson, P.-Å., Fellers, C., and Terland, O.; "Fibre orientation and its relation to paper formation studied by image analysis", *Proc. Tappi 1987 Paper Physics Conf.*, 185 (1987).
23. Wahjudi, U., Duffy G. G., and Kibblewhite, R. P.; "An evaluation of three formation testers using radiata pine and spruce kraft pulps", *Appita J.*, **51** (6) : 423 (1998).
24. Kajanto, I. M., Komppa, A., and Ritala, R. K.: "How formation should be measured and characterised", *Nordic Pulp and Paper Res J.*, **4** (3) : 219 (1989).
25. Odell, M. H., "Paper structure engineering" *Proc. 53rd Appita Annual Conf.*, Vol. I., 155 (1999).
26. Kiviranta, A. and Dodson, C.T.J. Dodson; "Evaluating Fourdrinier Formation Performance", *Jour Pulp & Paper Science*, **21** (11): 379 (1995).

**Appendix A: THK Data.**

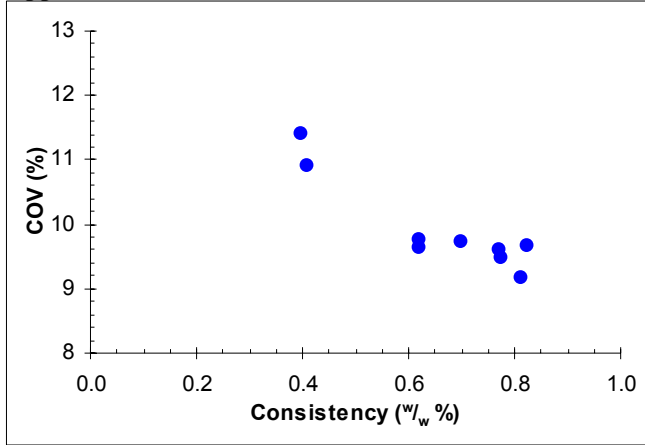


**Figure A1: COV of THK sheets at  $\bar{v} = 0.5$  m/s and various consistencies, ( $h = 10$ mm,  $\Delta P_{vac} = -8$ kPa).**

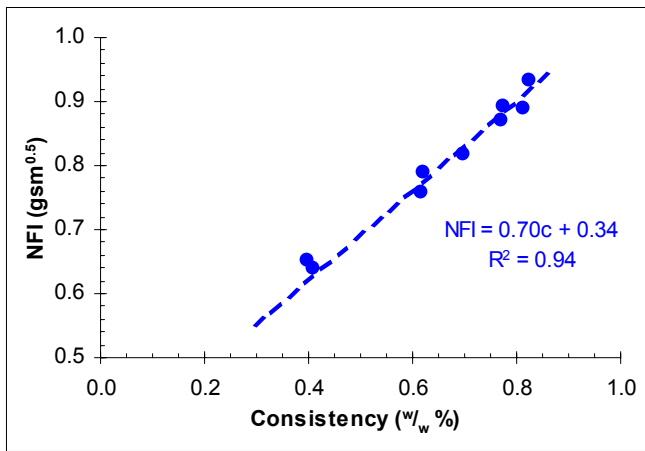


**Figure A2: NFI of THK sheets at  $\bar{v} = 0.5$  m/s and various consistencies, ( $h = 10$ mm,  $\Delta P_{vac} = -8$ kPa).**

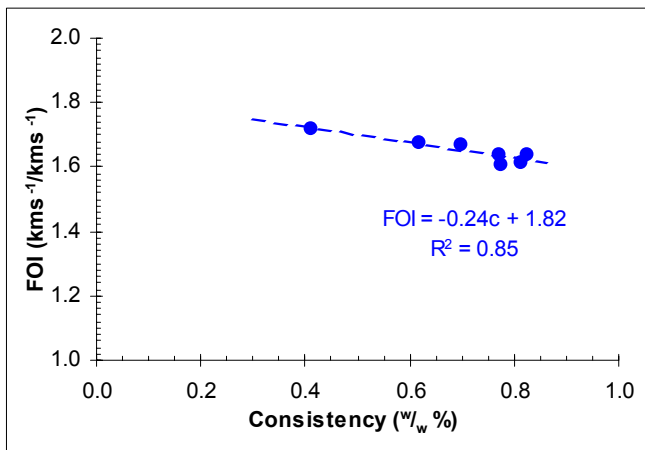


**Figure A3: FOI of THK sheets at  $\bar{v} = 0.5$  m/s and various consistencies, ( $h = 10$ mm,  $\Delta P_{vac} = -8$ kPa).**

In the following figures, A4 - A6, the sheet represented by the hollow point was formed at  $\bar{v} = 0.7$  m/s.

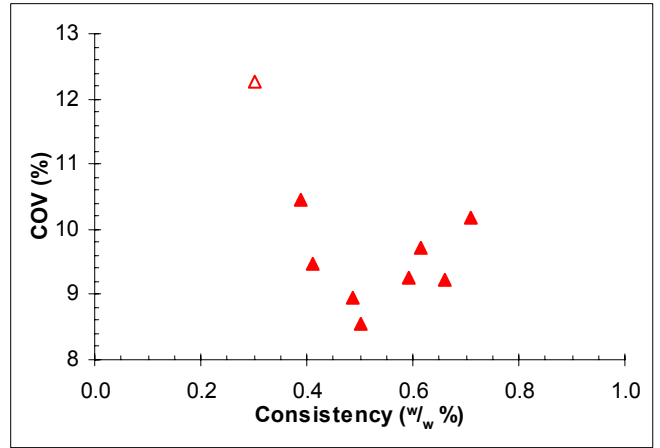


**Figure A4: COV of THK sheets at  $\bar{v} = 0.63$  m/s and various consistencies, ( $h = 10$ mm,  $\Delta P_{vac} = -8$ kPa).**

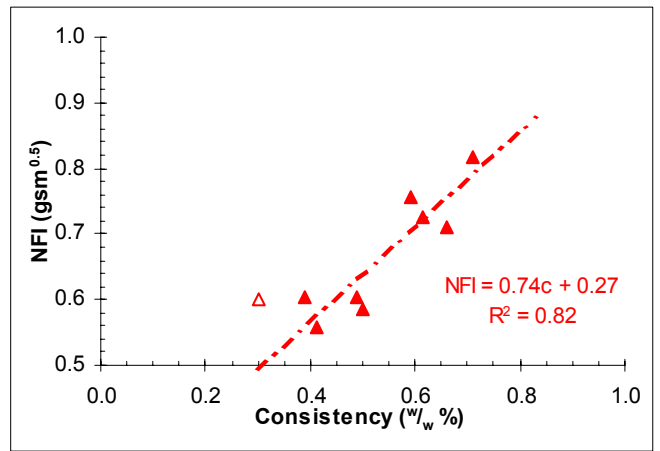


**Figure A5: NFI of THK sheets at  $\bar{v} = 0.63$  m/s and various consistencies, ( $h = 10$ mm,  $\Delta P_{vac} = -8$ kPa).**

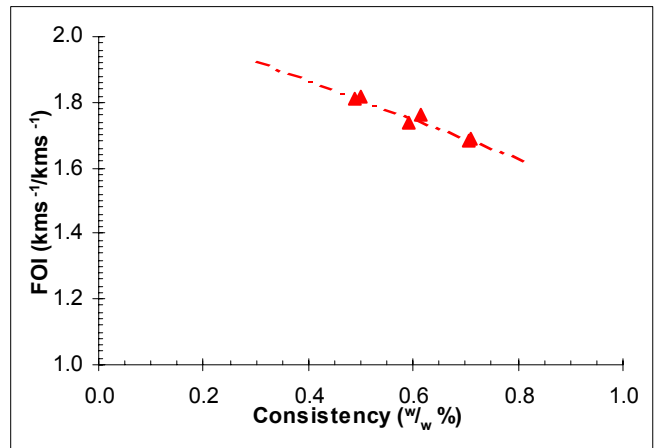


**Figure A6: FOI of THK sheets at  $\bar{v} = 0.63$  m/s and various consistencies, ( $h = 10$ mm,  $\Delta P_{vac} = -8$ kPa).**

**Table A1**

**Low velocity sheets, ( $h = 10$ mm,  $\Delta P_{vac} = -8$ kPa).**

c w/w %	v m/s	COV %	NFI gsm <sup>0.5</sup>	FOI kms <sup>-1</sup> /kms <sup>-1</sup>
0.40	0.30	11.94	0.77	1.53
0.41	0.30	12.8	0.82	1.53